

Temporal Human Action Segmentation via Dynamic Clustering

Yan Zhang

Institute of Neural Information Processing, Ulm University, Germany

yan.zhang@uni-ulm.de

He Sun

School of Informatics, The University of Edinburgh, UK

h.sun@ed.ac.uk

Siyu Tang

Department of Perceiving Systems, Max Planck Institute for Intelligent Systems, Germany

The University of Tübingen, Germany

stang@tuebingen.mpg.de

Heiko Neumann

Institute of Neural Information Processing, Ulm University, Germany

heiko.neumann@uni-ulm.de

March 20, 2018

Abstract

We present an effective dynamic clustering algorithm for the task of temporal human action segmentation, which has comprehensive applications such as robotics, motion analysis, and patient monitoring. Our proposed algorithm is unsupervised, fast, generic to process various types of features, and applicable in both the online and offline settings. We perform extensive experiments of processing data streams, and show that our algorithm achieves the state-of-the-art results for both online and offline settings.

1 Introduction

Automatic analysing human behaviours in a video stream is an important step for building an intelligent system that can perceive and interact with humans as humans do. It closely relates to many computer vision tasks, such as video summarisation, segmentation of human motion sequences [37], and detection of unusual activities [35], which have received a lot of attention in recent years.

Most of previous algorithms for analysing human behaviours are based on supervised learning, in which a large amount of training sets are required and human behaviours in each training set need to be labelled manually. In addition, most supervised learning approaches focus on the offline setting, producing the result after processing an entire video. While the performance of such supervised approach also relies on the quality of annotation and the irregularity in the periodicity of human actions, for many important applications like health-care and surveillance the training sets are usually not publicly accessible for data privacy reasons. Thus, developing an unsupervised and data-driven approach to analysing human behaviours is of great interest.

In this work we propose a fast and dynamic clustering algorithm to process a generic multi-dimensional time series. As the output of our algorithm, the clusters are formed in a data-driven fashion and evolve dynamically over time, see Figure 1 for illustration. More specifically, our algorithm consists of two steps: (1) In the initialisation step, we utilise a robust spectral clustering method [20, 22] to learn the centers and the covariances of the initial patterns in an unsupervised fashion. These basic statistics, including the centers and covariances of the clusters, are associated with the spatial concentration/separation properties of the same/different human actions of feature vectors, and are used to predict new human actions; (2) in the online evolution step, the algorithm either treats every arriving feature vector as one of the existing actions or recognises it as a new

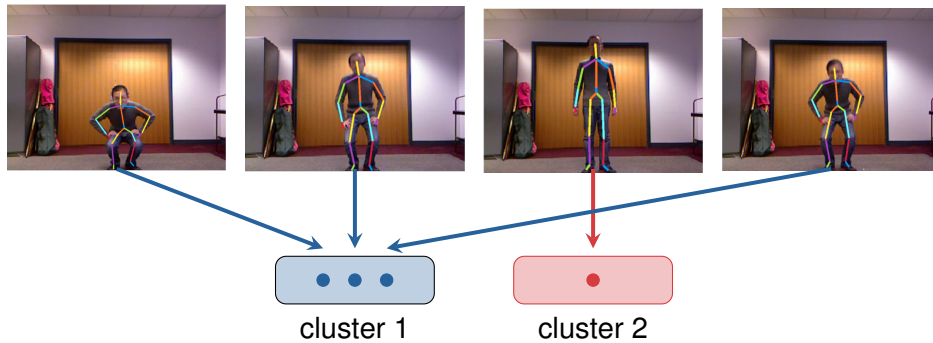


Figure 1: Illustration of our approach. Our algorithm updates the clustering structure dynamically, and performs the dynamic segmentation task based on the transition point from which two consecutive feature vectors belong to different clusters.

action, and further updates the center and covariance information of an existing or new cluster. Due to the ability of effectively extracting statistical information of feature vectors, our algorithm is able to process video streams from generic multi-dimensional time series and different kinds of features.

We perform a number of experiments for the proposed algorithm, and compare it with the state-of-the-art. For instance, when applying the `JointLocation` features to the `CMUMAD` dataset [9], our method achieves 0.82/0.86 precision/recall value within 0.1 seconds in the offline setting. The classical offline `Aligned Cluster Analysis (ACA)` algorithm [37] achieves 0.55/0.68 precision/recall value, but its runtime is 2,200 times slower than ours.

We further evaluate our algorithm on more complicated `TUMKitchen` [29] and `HDM05` [19] datasets: for various feature vectors applied, our algorithm achieves better or similar precision/recall values but runs significantly faster than the state-of-the-art.

2 Related Work

Temporal action segmentation is an important research topic with applications in robotics, machine learning, computer vision, etc. The model-based approach for solving this problem relates to action detection, which is usually addressed by training discriminative or generative models [21, 15, 17, 24, 25, 28, 34, 14]. These methods require either a large amount of training data with annotations which introduces high computation cost, or the collection of training sets and an offline learning step, e.g., [2, 13]. In contrast, unsupervised clustering-based methods parse actions into motion primitives only based on the processed data stream, and hence can be used in many important scenarios in which training sets are not publicly available, e.g., health-care and surveillance.

[36] proposes `aligned cluster analysis (ACA)` that uses a novel kernel for time series alignment. After specifying the number of clusters, as well as the minimum and maximum lengths of the action segments, both the `ACA` and `HACA`, an improved version of `ACA`, solve a dynamic program over the entire stream, which makes both approaches non-applicable for fast and online video segmentation. [12] proposes an efficient motion segmentation approach, in which a novel feature bundling method is used to generate compact and robust motion representations. In particular, a generalised search radius is introduced in [12] so that the number of clusters is not needed as input. [16] addresses motion segmentation via subspace clustering, in which a temporal Laplacian regularisation method is applied to encode the temporal structure in the subspace and spectral clustering is applied to group actions using the projected feature vectors.

Another related line of research is the mixture model for clustering, which can be trained online. [30] proposes a greedy method for training the Gaussian mixture model, but requires to specify the model complexity, e.g., the number of clusters k , in advance. To overcome this, the Bayesian nonparametric models learn the value of k from the input data jointly with the observation models. For example, `Dirichlet process mixture model (DPMM)` [1, 6] uses a `Dirichlet process` to allocate samples and calculate k , where the joint probabilities of allocations are independent of the temporal order of the input samples. [10] proposes an algorithm to train `DPMM` by iteratively processing data batches and allowing the number of clusters varying when the model

parameters are updated online.

Our work differs from all these previous methods. Most previous studies formulate the human action segmentation via some optimisation problem, and apply dynamic programming or spectral techniques to solve the problem. These techniques usually require the global information of the dataset and have high computational cost, in contrast to our greedy and online approach. Comparing our approach with DPMM, one should notice that DPMM is based on keeping track of some probabilistic distributions, while our algorithm keeps track of some geometric measure associated with the input.

Regarding the online setting, [7] proposes Kernelised Temporal Cut (KTC) to sequentially cut a video stream into different snippets, and develops an online algorithm to locate segment boundaries. [8] proposes an approach to learning the temporal regularity based on the autoencoder. Then the local minima of the regularity scores can be regarded as action transitions. Our work differs from these mentioned online methods: They perform segmentation based on changing point detection while our method is based on online clustering. Thus, our algorithm produces a *clustering* of the segmented snippets, and the output of our algorithm can provide more semantic meaning than other online approaches.

3 Algorithm

Now we present our dynamic clustering method for segmenting human actions, which refers to the task of dividing a video stream into disjoint snippets so that every snippet presents a single action. This problem is closely related to partitioning the associated feature vectors into clusters such that the feature vectors in each cluster represent a single human action.

Formally, we assume that we are given a sequence of vectors $\mathbf{x}_1, \dots, \mathbf{x}_t, \dots$ as input, in which every $\mathbf{x}_i \in \mathbb{R}^d$ is the feature vector at time i . The goal is to find cut points (the transition timestamps), such that different human actions are separated by these cut points. To make our approach applicable in realistic scenarios, we do not make additional assumptions on the input feature vectors, in the sense that each new arriving input \mathbf{x}_i could be either a feature vector corresponding to a single frame or a video snippet (e.g., a Fisher vector [13, 32] can represent the context of 50 frames).

3.1 Our Approach

The design of our algorithm is based on the fact that the feature vectors representing the same human actions are similar to each other, although a “quantitative” measurement of this similarity usually depends on the nature of the feature vectors, including the dimensionality, the spatiotemporal scales, and how a feature vector is generated, etc. To deal with this fact, our algorithm first computes the basic statistics of the input feature vectors, which is achieved by building a fully connected similarity graph G from the initial feature vectors of a fixed-length sliding window and running a spectral clustering algorithm on G , where the number of clusters k is determined by the graph spectra [31]. Comparing with a classical spectral clustering algorithm that only gives a partition of the vertices of G , our algorithm computes the centers $\{\mathbf{c}_i\}_{i=1}^k$ of the clusters to measure *how far clusters are separated from each other*, and diagonal matrices $\{\Sigma_i\}_{i=1}^k$, each of which is associated with one cluster and measures *how concentrated all the feature vectors within each cluster are around the center*. We define the cluster set \mathcal{C} as the combination of $\{\mathbf{c}_i\}_{i=1}^k$ and $\{\Sigma_i\}_{i=1}^k$. The length of the time window is dependent on a specific application, in order to cover the representative statistics of the entire time series.

Afterwards, our algorithm enters the updating phase and runs in an online fashion: for every arriving vector \mathbf{x}_t , the algorithm computes the distance between \mathbf{x}_t and its closest center of all the observed clusters $\mathbf{c}_1, \dots, \mathbf{c}_k$, i.e., $\text{dist}(\mathbf{x}_t, \mathcal{C}) = \min_{1 \leq i \leq k} \|\mathbf{x}_t - \mathbf{c}_i\|^2$. Based on $\text{dist}(\mathbf{x}_t, \mathcal{C})$ and matrices $\{\Sigma_i\}$, the algorithm decides whether to put \mathbf{x}_t into its closest cluster, or generates a new cluster to host \mathbf{x}_t . Notice that the runtime of this step is only proportional to the number of currently observed clusters and the dimension of the feature vectors, which is independent of the length of the video stream. Hence, the update time for every arriving feature vector can be accomplished in $O(1)$ for most applications.

3.2 Initialisation Step

The input of the initialisation step are the initial ℓ feature vectors $\mathbf{x}_1, \dots, \mathbf{x}_\ell$ from a video stream. The algorithm first constructs a fully connected graph $G = (V, E)$ of ℓ vertices, denoted by v_1, \dots, v_ℓ , where

each v_i corresponds to a vector \mathbf{x}_i and the weight of the edge between v_i and v_j is defined as $w(v_i, v_j) = \exp(-\|\mathbf{x}_i - \mathbf{x}_j\|^2/\sigma)$ with a parameter σ . This graph G is represented by the normalised Laplacian matrix, which is defined by $\mathcal{L} = \mathbf{I} - \mathbf{D}^{-1/2}\mathbf{A}\mathbf{D}^{-1/2}$, where $\mathbf{I} \in \mathbb{R}^{\ell \times \ell}$ is the identity matrix, $\mathbf{D} \in \mathbb{R}^{\ell \times \ell}$ is the diagonal matrix defined by $\mathbf{D}_{i,i} = \sum_j w(v_i, v_j)$, and $\mathbf{A} \in \mathbb{R}^{\ell \times \ell}$ is the adjacency matrix of G . We then compute the eigenvalues $\lambda_1 \leq \dots \leq \lambda_\ell$ of \mathcal{L} , and use the smallest value k with a large gap between λ_{k+1} and λ_k to determine the number of clusters. This method is widely used for determining the number of clusters in practice, see [22] for theoretical explanation and [31] for detailed discussion.

After computing the value of k , the algorithm runs k -means for the initial ℓ feature vectors $\mathbf{x}_1, \dots, \mathbf{x}_\ell$. In addition to the k clusters produced by k -means, the following quantities are computed: (1) Centres $\{\mathbf{c}_i\}_{i=1}^k$ for these k clusters; (2) Covariance matrices $\{\Sigma_i\}_{i=1}^k$, where $\Sigma_i \triangleq \mathbf{diag}\left(\left(\sigma_1^{(i)}\right)^2, \dots, \left(\sigma_d^{(i)}\right)^2\right)$ and $\sigma_j^{(i)}$ is defined as the ℓ_2 -distance of the j th coordinate between all the feature vectors in the i th cluster and their center; (3) Radiuses $\{r_i\}_{i=1}^k$ for the k clusters and defined by $r_i \triangleq \text{Tr} \Sigma_i$. Moreover, we define a minimum area of the cluster δ_r with $\delta_r \triangleq c \cdot d$, which is similar to the search radius introduced in [12]. The constant c is a hyper-parameter, which can be viewed as the uncertainty estimate of each dimension, and is empirically determined depending on the use.

3.3 Online Evolution Step

The second step of our algorithm is the online clustering based on the statistical information of the currently observed clusters. Specifically, for every arriving \mathbf{x}_t the algorithm computes the distance between \mathbf{x}_t and its closest center, i.e., $\text{dist}(\mathbf{x}_t, \mathcal{C}) = \min_{1 \leq i \leq k} \|\mathbf{x}_t - \mathbf{c}_i\|^2$. Depending on such distance, the algorithm either creates a new cluster consisting of a single point \mathbf{x}_t , or adds \mathbf{x}_t to its closest cluster and updates the corresponding \mathbf{c}_i and Σ_i . The formal description is presented in Algorithm 1. Here, \circ denotes the Hadamard product operation. Notice that, for the task of online segmentation, a transitional point is detected if the current observed \mathbf{x}_t and \mathbf{x}_{t-1} belong to different clusters.

Algorithm 1 Online Evolution Step

- 1: $\text{dist}(\mathbf{x}_t, \mathcal{C}) = \min_{1 \leq i \leq k} \|\mathbf{x}_t - \mathbf{c}_i\|^2$.
 $i^* = \arg \min_{1 \leq i \leq k} \|\mathbf{x}_t - \mathbf{c}_i\|^2$.
 - 2: **if** $\text{dist}(\mathbf{x}_t, \mathcal{C}) \geq \max\{r_{i^*}, \delta_r\}$ **then**
 $k \leftarrow k + 1$; $S_k \leftarrow \{\mathbf{x}_t\}$;
 $\mathbf{c}_k \leftarrow \mathbf{x}_t$; $M_k \leftarrow \mathbf{x}_t \circ \mathbf{x}_t$;
 $\Sigma_k \leftarrow \mathbf{diag}(0, 0, \dots, 0)$.
 - 3: **else**
 $\mathbf{c}_{i^*} \leftarrow \mathbf{c}_{i^*} + (\mathbf{x}_t - \mathbf{c}_{i^*}) \cdot |S_{i^*}|^{-1}$;
 $M_{i^*} \leftarrow (M_{i^*} \cdot |S_{i^*}| + \mathbf{x}_t \circ \mathbf{x}_t) / (|S_{i^*}| + 1)$;
 $\Sigma_{i^*} \leftarrow M_{i^*} - \mathbf{c}_{i^*} \circ \mathbf{c}_{i^*}$;
 $r_{i^*} \leftarrow \text{Tr} \Sigma_{i^*}$; $S_{i^*} \leftarrow S_{i^*} + \{\mathbf{x}_t\}$.
-

3.4 Runtime Analysis

For the initialisation step, we first need to build the similarity graph based on ℓ feature vectors, each of which has dimension d . This takes $O(\ell^2 \cdot d)$ time. After that, computing all the eigenvalues of matrix \mathcal{L} takes $O(\ell^3)$ time, and $O(\ell \cdot k)$ time is needed for writing down the spectral embedding of all the vertices. After this, we can apply a polynomial-time approximation scheme (PTAS) algorithm for the k -means clustering problem with runtime $O\left(\ell \cdot k^2 + 2^{\tilde{O}(k)}\right)$ when treating the approximation parameter ε involved in the definition of PTAS as $\varepsilon = \Omega(1)$, [5]. Since the number of clusters $k = O(1)$ for most applications, this step takes $O(\ell^2 \cdot d + \ell^3)$ time.

For the online evolution step, computing the distance between every arriving \mathbf{x}_t and its closest center takes time $O(k \cdot d)$, where k is the number of clusters at time t . After that, $O(d)$ time suffices to update all the quantities maintained by the algorithm. Hence, the update time for each arriving feature vector is $O(k \cdot d)$.

3.5 Further Discussion

At the end, we briefly discuss our algorithm in comparison to online k -means clustering, which has received considerable attention in theoretical computer science and machine learning. It has been observed in [18] that any online k -means algorithm with bounded approximation guarantee has to generate strictly more than k clusters, due to the following fact:

Assume all the data points are in \mathbb{R} , $k = 2$, and the first two arriving points are $v_1 = 0$ and $v_2 = 1$, respectively. At this point any algorithm will put v_1 and v_2 into two clusters with total cost 0, since otherwise putting them into a single cluster will increase the cost value from 0 to $1/2$. However, after an algorithm assigns v_1 and v_2 to different clusters, the third arriving point could be $v_3 = c$ for an arbitrary large value c . At this stage, the algorithm is forced to put v_3 into one of the two existing clusters, which makes the total cost at least $\Omega(c)$ in contrast to the optimal cost value $1/2$. It is straightforward to generalise this example to the case of $k \geq 3$ clusters in high-dimensional space, which explains why online k -means algorithms cannot be applied to solve our problem.

However, our key observation is that, a combination of determining the value of k via graph spectra and a variant of k -means could work well for human action detection. To explain the reason, we look at the task of online clustering points $\mathbf{x}_1, \dots, \mathbf{x}_n \in \mathbb{R}^d$ into k clusters with the following two extreme cases, where these k clusters are far from each other. (i) When the points associated with each cluster arrive together, it's not difficult to find a nearly-optimal clustering; (ii) the task becomes challenging when the k points from k different clusters arrive first, since whether grouping them into k or fewer clusters depends on the locations of the remaining $n - k$ points, i.e., the worst-case example for online k -means discussed above. Remarkably, for online human action detection we do not need to consider (ii) since graph spectra allow us to learn the geometry of the initial data points, e.g., how they're concentrated around the centers. Moreover, due to the physical continuity of human motions, the temporal structure of a feature sequence is smooth and an algorithm will receive many points around a center, before receiving points from another cluster, and the statistical information of the initial clusters can be usually generalised to new clusters. Such temporal coherence characteristic is also considered in other tasks, e.g. [33, 11]. Hence, it suffices to consider the scenario similar to (i). This explains why our algorithm works in theory, and the worst-case scenario for online k -means is successfully avoided through an application of the eigengap heuristic [31].

4 Offline Action Segmentation

We experimentally compare our algorithm with the state-of-the-art when various features are applied as input. Our experiments are conducted on a computer equipped with Intel Core i7-6700K 4GHz 8-core processors, the Geforce GTX 1080 graphics card, and 32GB RAM. The operating system is Ubuntu 16.04. Our proposed algorithm is implemented with C++ and compiled in Matlab R2017a. The source code of our algorithm will be published online after the double-blind review process.

4.1 Datasets

Our algorithm will be evaluated on the following three datasets:

- The CMUMAD dataset [9] contains 40 recordings from 20 subjects, and covers comprehensive body action types from three modalities: RGB video and 3D depth map with spatial resolution of 240×324 of pixels, and the 3D body skeleton with 20 joints per frame. Each recording is about 2 – 4 minutes, and consists of 35 actions which are performed continuously. A null action (standing) is performed between consecutive actions.
- The TUMKitchen dataset [29] consists of 20 recordings from multiple modalities. The camera network captures the scene from four viewpoints with 25 fps, and every RGB frame is of the resolution 384×288 by pixels. The action labels are frame-wise, and provided for the left arm, the right arm and the torso separately.
- The HDM05 dataset [19] is a large motion capture dataset containing more than 3 hours of human motion recordings. In our experiments we use the third category, i.e., *Sports*, which is significantly more

challenging than the other categories. The *Sport* category incorporates motion recordings from 11 sports classes, each of which contains approximate 50000 – 100000 frames.

4.2 Feature Extraction

We use five types of features from different modalities, aiming to represent actions from a comprehensive set of information sources. The first two are context-based features, and the other three are pose-based features:

- **IDT+FV**: In our experiment the motion boundary histogram is extracted around the dense trajectories of all scales [32]. The Gaussian mixture model with 32 components is trained using the other video performed by the same person, and vice versa. If the amount of motion boundary histograms is larger than 10^6 , only 10^6 of them are selected randomly to train the Gaussian mixture model. Instead of encoding an entire video, we use a sliding window scheme to aggregate temporally local features. The time window spans 50 frames and the stride is 1. The resulting Fisher vector has 12, 288 dimensions.
- **VGG16**: We use the two stream deep neural model VGG-16 [26, 4] which is pre-trained on the UCF101-Split1 dataset [27], and extract the output of the last fully-connected layer. Since the colour channel and the motion channel are separate, we concatenate the outputs from both channels to compose a feature of 202 dimensions for our experiments. Due to the model architecture, the VGG16 feature describes the context in a snippet of 10 frames.
- **JointLocation**: We concatenate all the 3D coordinates of the joints to form a feature of each individual frame. Such feature can be viewed as an unary representation of a body configuration.
- **RelativeAngle**: We use the relative 2D angle between two adjacent body components to represent the rotation. This feature can be viewed as a high-order representation of the body configuration and possesses rotational invariance.
- **Quaternions**: Like in [7], we use the quaternions to represent the 3D rotation of a joint. Due to the ability of representing 3D rotations, the quaternion feature provides richer information than **RelativeAngle**.

Feature Aggregation. Since features that only encode information of one or a few frames are not sufficient to encode actions, we apply feature aggregation to derive action patterns from temporally local features. Feature aggregation consists of two steps: feature encoding, and temporal pooling. For feature encoding, we view the output of our algorithm as codebook and encode each individual local feature using soft assignment [23]. To perform temporal pooling, we define several temporal windows, fuse (add and normalize) the encoded features within each temporal window and obtain the action patterns. Afterwards, action segmentation is obtained by simply performing k -means on such action patterns.

We use different temporal pooling approaches for different datasets. In each recording CMUMAD, the null action comes first and repeatedly occurs between each two actions. We assign the label 0 to the frames that belong to the same cluster with the first frame. Afterwards, we apply Gaussian smoothing on the temporal label sequence and detect all the peaks as well as their widths to create time windows. In contrast, as the TUMKitchen and HDM05 datasets do not have null actions, we use a sliding window scheme to perform temporal pooling, in which each time window consists of 30 frames and the stride is of 1 frame.

4.3 Results on the CMUMAD Dataset

We first introduce the experimental setup and the evaluation metrics. Then we present our experimental results and compare our algorithm with the state-of-the-art methods.

Evaluation Metric. The performance of all algorithms are evaluated based on precision-recall values [3], in which the true positive is commonly defined based on a region matching without considering the labels [12, 16]. Here we use a more critical definition to capture the semi-semantic meaning of the segmentations given by the clusters. We define a true positive as the segment within which the majority of the predicted labels have more than 50% overlaps with the ground truth labels, and this predicted label is not 0 and not predicated before.

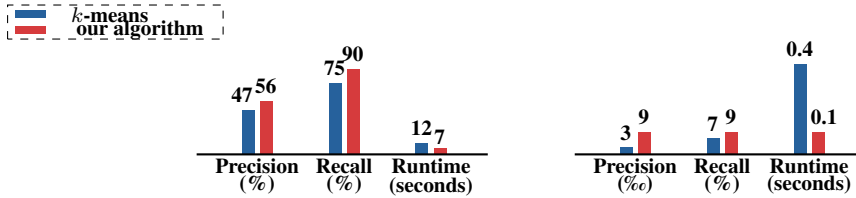


Figure 2: Comparison between our algorithm and k -means when applying IDT+FV with 12,288 dimensions and VGG16 with 202 dimensions as input.

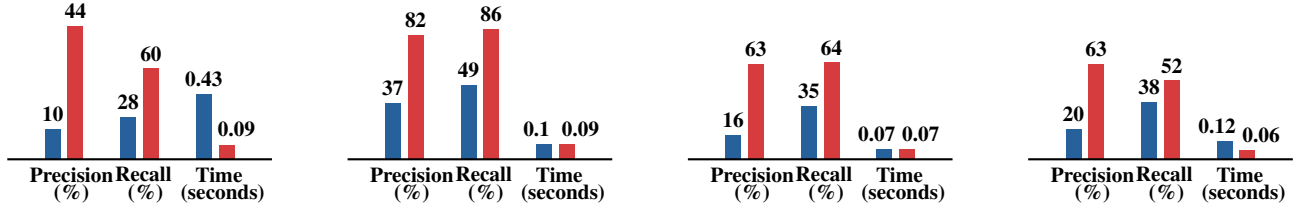


Figure 3: Comparison between our algorithm (red) with k -means (blue). Here, the four subfigures represent the comparison results when VGG16 (202 dimensions), JointLocation (60 dimensions), RelativeAngle (15 dimensions), and Quaternions (60 dimensions) are applied as feature vectors.

Hence the influence of null actions is excluded and each meaningful action can be regarded as a novel action. Moreover, we use runtime to measure the speed of segmentation algorithms, for which the feature extraction step is not considered. All the reported values are the average of the ones from all the recordings.

Analysis with snippet-wise features. We compare the performance of our algorithm with that of the classical k -means for snippet-wise features, without using the feature aggregation step for post processing. As shown in Figure 2, our algorithm runs much faster than k -means, and achieves better precision and recall values. Our experiments also indicate that both of our algorithm and k -means perform better when applying the IDT+FV features rather than VGG16 features: this is due to the fact that, while an IDT+FV feature presents a snippet of 50 frames, a VGG16 feature presents a snippet of 10 frames and is not sufficient to represent the actions spanning longer time.

Analysis with frame-wise features. We apply our clustering algorithm together with the feature aggregation step as post processing when frame-wise features are applied. Due to the experimental results before, we apply VGG16 features as input for our experiments here. The evaluation result is shown in Figure 3, which confirms again that with similar runtime our algorithm produces better results than k -means for all the tested features. Moreover, one can note that our algorithm runs much faster than k -means for high dimensional feature vectors.

Comparing with the state-of-the-art. We compare the performance of our algorithm with the following state-of-the-art methods:

- Spectral clustering (SC). We implement the standard spectral clustering algorithm, and set the parameter σ associated with the similarity graph to $\sigma = 1$. We also set $k = 36$, since the initial null action needs to be treated as a single cluster.
- Temporal subspace clustering (TSC) [16]. We use the default hyper-parameters specified in [16] for feature vectors of 100 dimensions. When the dimension of the input feature vectors is more than 100, we first apply PCA to project all the input features to \mathbb{R}^{100} .
- Aligned cluster analysis (ACA) [36]: We use the implementation of ACA provided by the authors of [36], in which the number of clusters is set to 36 and the minimal and maximal segment lengths are tuned

Table 1: Comparison between our method with state-of-the-art, where the results are given in format of *precision/recall/runtime*. The best results are highlighted in boldface, and the time needed for PCA is included in the reported runtime. Since the feature **IDT+FV** represents the content of 50 frames, feature aggregation is not applied

Algorithm	IDT+FV [32]	VGG16 [4]	JointLocation	RelativeAngle	Quaternions
SC	0.57/0.85/203.3	0.004/0.05/118.8	0.02/0.13/113.0	0.003/0.06/113.4	0.01/0.11/125.3
TSC [16]	0.63/0.82/132.4	0.01/0.2/38.2	0.1/0.3/48.5	0.05/0.29/41.6	0.05/0.29/38.7
ACA [36]	0.91 /0.83/547.7	0.56/0.66/99.0	0.55/0.68/221.5	0.51/0.65/136.2	0.55/ 0.66 /168.8
EMS [12]	0.44/0.75/78.4	0.67/0.73 /35.8	0.34/0.78/33.0	0.47/ 0.89 /17.3	0.6/0.51/9.2
DPMM [10]	0.4/0.73/507.8	0.009/0.08/8.6	0.02/0.12/17.8	0.02/0.1/13.4	0.02/0.11/11.6
DPMM-A	n/a	0.24/0.53/8.6	0.37/0.54/17.8	0.27/0.5/13.4	0.39/0.58/11.6
ours	0.56/ 0.97/7.0	0.44/0.6/ 0.1	0.82/0.86/0.1	0.63/0.64/0.1	0.63/0.52/0.1

based on the CMUMAD dataset. We remark that we do not compare our algorithm with the hierarchical ACA algorithm (HACA), because of much higher computational cost and hyper-parameter tuning for the latter algorithm. Moreover, the ACA algorithm with the IDT+FV is computationally prohibitive. Thus, we first use PCA to project the Fisher vectors to \mathbb{R}^{100} as well.

- Efficient Motion Segmentation (EMS) [12]: We tune the hyper-parameters to achieve the best performance with each feature. In addition, due to high computational load for IDT+FV, we first use PCA to project the Fisher vectors to a 100-dimensional subspace.¹
- Dirichlet Process Mixture Model (DPMM) [10]. We use the method proposed in [10] to train the DPMM, and set the allocation model as the Dirichlet process and the observation model as a Gaussian distribution with the diagonal covariance matrix. We denote DPMM-A as the combination of DPMM and our proposed feature aggregation method.

The comparison results are shown in Table 1: SC, TSC and DPMM are to assign each sample from a video stream to an *action cluster* directly, and hence perform better when grouping action patterns (**IDT+FV**) than the other temporally local features, which lacks of representativeness of actions. Instead, ACA and EMS consider the similarities of feature vectors over a long period of a video stream, which makes the output of ACA and EMS algorithms more consistent when different types of features are applied. One can also clearly see that feature aggregation, which converts temporally local features to long-term segment patterns, boosts the performance of action segmentation when the temporally local features are applied as input, as shown in the results of DPMM and DPMM-A. When comparing our algorithm with the state-of-the-art, one can see that our algorithm runs hundreds of times faster than other algorithms but produces comparable results with ACA. In particular, when the JointLocation features are applied, our algorithm produces the best results among all the tested algorithms, which is illustrated in Figure 4.

4.4 Results on the TUMKitchen and HDM05 Datasets

We report our experimental results on the TUMKitchen and HDM05 datasets, which contain more realistic and complex movements.

Evaluation metric. The TUMKitchen and HDM05 datasets have no null actions and the performed actions might occur more than once, hence the strict evaluation metric used in the CMUMAD dataset is not suitable here anymore. To cope with this, we redefine the true positive in the precision-recall metric: we say that a ground truth boundary is correctly detected if the detected boundary by an algorithm is within ± 7 frames (about ± 0.25 second) of the ground truth boundary. The reported values are the average of the experimental results from all recordings.

¹The codes provided by the authors of [12] are implemented at Windows-64 operating system, and therefore this approach is tested on a computer equipped with Intel Core i7-6700HQ CPU at 2.6GHz and 16GB RAM.

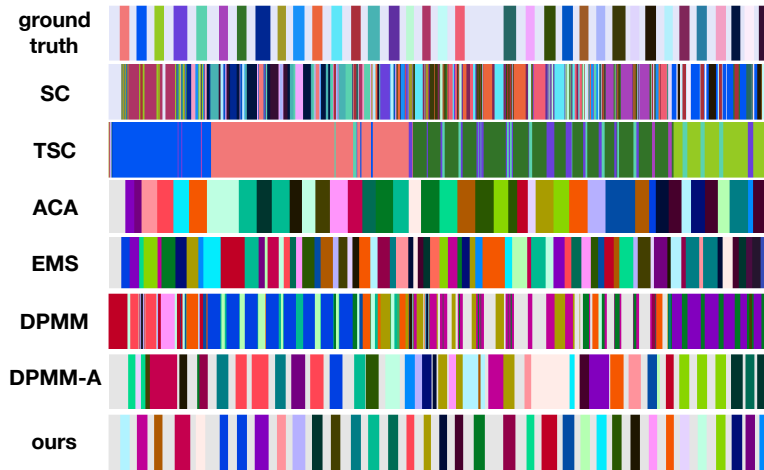


Figure 4: Visualised segmentation result of the compared algorithms. Here, the input is the first recording of Subject 5 of the dataset, and JointLocations features are employed.

Comparing with the state-of-the-art. For the TUMKitchen dataset, action labels are annotated by individual body parts instead of an entire body. Therefore, we only apply the pose-based features (JointLocation, RelativeAngle and Quaternions) and perform segmentation for individual body parts. Since the left arm and the right arm have symmetric dynamics, we evaluate the two arms jointly. The detailed comparison results are shown in Table 2, from which one can see that our algorithm runs much faster than the others but produces better/comparable results, which was confirmed by our experiments for the CMUMAD dataset.

Table 2: Results on the TUMKitchen dataset, where the results are shown in format of *precision/recall/runtime* and the best results are shown in boldface

Algorithm	Type	JointLocation	RelativeAngle	Quaternions
SC	Torso	0.02/0.01/9.1	0.24/0.28/8.6	0.3/0.45/8.7
	Arms	0.29/0.47/8.8	0.17/ 0.82 /8.8	0.18/ 0.76 /8.6
TSC	Torso	0.12/0.04/10.1	0.28/0.1/10.2	0.31/0.19/10.1
	Arms	0.42/0.28/10.2	0.29/0.38/10.3	0.28/0.56/10.2
ACA	Torso	0.19/0.01/30.5	0.3/0.02/15.6	0.4 /0.03/24.6
	Arms	0.36/0.08/24.6	0.36/0.1/19.6	0.34 /0.09/26.1
EMS	Torso	0.13/0.06/4.6	0.28/0.15/35.4	0.37/0.12/11.5
	Arms	0.26/0.12/5.4	0.38 /0.27/12.7	0.34 /0.09/8.4
DPMM	Torso	0.27/ 0.66 /11.1	0.18/ 0.63 /11.3	0.30/ 0.55 /3.3
	Arms	0.33/ 0.52 /10.2	0.12/0.54/2.0	0.22/0.27/4.9
DPMM-A	Torso	0.23/0.15/11.1	0.36/0.16/11.3	0.37/0.19/3.3
	Arms	0.31/0.41/10.2	0.23/0.58/2.0	0.24/0.46/4.9
ours	Torso	0.46 /0.15/ 1.0	0.34 /0.12/ 0.3	0.4 /0.26/ 1.3
	Arms	0.49 /0.3/ 1.0	0.27/0.64/ 1.0	0.33/0.68/ 0.3

For the HDM05 dataset, we use the pose-based features as the HDM05 dataset only contains motion capture data. Our experimental results are shown in Table 3, and confirm once more about the performance of our algorithm over the state-of-the-art. We highlight that, on both TUMKitchen and HDM05 datasets our algorithm yields much better recall values than ACA. A probable reason is that our algorithm compares each frame with previous ones, which leads to higher temporal resolution than the segment comparison in ACA and hence is able to locate the segment boundary more precisely.

5 Online Action Transition Detection

In this section, we compare our method with the state-of-the-art online methods. In such action transition detection task, the algorithm locates a segment boundary at the current time, if the current frame belongs to a

Table 3: Experimental results on Part-Scene 3 (Sports) of HDM05

Algorithm	JointLocation	RelativeAngle	Quaternions
SC	0.15/ 0.36 /88.6	0.11/ 0.32/145.2	0.14/ 0.37 /145.9
TSC	0.16/0.29/46.5	0.13/0.2/59.8	0.14/0.28/74.2
ACA	0.11/0.04/443.3	0.17 /0.07/382.8	0.13/0.05/343.3
EMS	0.17 /0.11/6.3	0.11/0.1/26.6	0.14/0.11/16.5
DPMM	0.1/0.24/23.1	0.07/0.1/7.5	0.13/0.27/16.3
DPMM-A	0.11/0.16/23.1	0.07/0.15/7.5	0.15 /0.23/16.3
ours	0.15/ 0.23/ 1.0	0.11/ 0.33 / 1.3	0.15 /0.27/ 1.3

different cluster from the previous frame. Due to frame-by-frame processing in the online setting, the feature aggregation step is disabled.

Evaluation metric. We use the same evaluation metric as in Sec. 4.4. Since the task online is more time-sensitive, the temporal range to define the true positive is set to be ± 2 frames (± 0.04 second).

Dataset and feature extraction. We use the TUMKitchen dataset for experiment. Comparing with CMU-MAD and HDM05, it has more realistic movements, multi-modal recordings, and separate annotations on the torso and the arms. These properties are suitable for analysing complex movements of individual body parts from multiple information sources. Besides the three pose-based features, we also use the contextual information from the video recordings.

Comparing with the state-of-the-art. We compare the performance of our algorithm with the following state-of-the-art online methods:

- Sequential kernelized temporal cut (KTC-S) [7]. The KTC-S is a method for segmenting human actions online. Here, we set every time window to be 25 frames, and use the degenerated version². The hyper-parameters of KTC-S are selected experimentally in order to achieve the best performance.
- Autoencoder with temporal regularity (ATR) [8]. In [8] the regions with high reconstruction errors (low regularity scores) are treated as abnormalities. Here we assume that human motions at action transitions violate the temporal regularity and extend the original offline local minima searching method to an online version, using the same sliding window method with KTC-S. Due to its generability, we directly use the provided model from [8].

Results and discussion. From Table 4, one can see that our algorithm produces comparable precision values but much higher recall values than other methods. We claim that in the online setting the recall is more important than precision for many applications (e.g., healthcare and surveillance) which require online and effectively detecting potential fast and abnormal actions. It is also noticeable that all the tested online algorithms suffer from over-segmentation issues and hence cause low precision values.

6 Conclusions

To cooperate with insistent need of processing data streams, we propose a dynamic algorithm for segmenting and clustering human actions. Comparing with previous methods, our algorithm is fast, generic for various features and also improves the state-of-the-art offline approaches when combining with a feature aggregation step. We experimentally evaluate our algorithm against the state-of-the-art methods on the standard datasets when different features are applied as input: for all the tested datasets, our algorithm produces better/comparable results but runs much faster than the state-of-the-art. Moreover, in the important scenario of online human

²We did not implement the full version of the algorithm proposed in [7] due to lack of information provided in the paper.

Table 4: Comparison between our algorithm and the state-of-the-art. The results are in format of *precision/recall* and the best values are highlighted in boldface. One notice that ATR extracts features from videos rather than poses. We show the results under the pose-based features only for comparison

Algorithm	Type	JointLocation	RelativeAngle	Quaternions
KTC-S	Torso	0.08 /0.36	0.08 /0.31	0.10 /0.40
	Arms	0.12 /0.38	0.13 /0.39	0.14 /0.42
ATR	Torso	0.06/0.29	0.06/0.29	0.06/0.29
	Arms	0.10/0.30	0.10/0.30	0.10/0.30
ours	Torso	0.07/ 0.62	0.08/0.49	0.08/ 0.50
	Arms	0.10/ 0.39	0.11/ 0.41	0.08/ 0.46

action segmentation, with comparable precision value our algorithm presents a significant improvement over the state-of-the-art with respect to recall value, which is more important for many applications.

Our work leaves many interesting problems for further research from both theoretical and applicational perspectives and we mention two questions here: (1) Theoretical studies for the connection between human action segmentation and clustering. Since clustering human actions requires to group feature vectors representing the same human action, it seems to be more challenging than setting segment boundaries. However, our proposed clustering algorithm achieves better results than the state-of-the-art for the segmentation task. We believe that this direction worths further studies under different setups. (2) online abnormal detection of human behaviours. The two questions are of wide interest not only for researchers working in computer vision and machine learning, but also for cognitive psychologists.

References

- [1] D. M. Blei and M. I. Jordan. Variational inference for dirichlet process mixtures. *Bayesian analysis*, 1(1):121–143, 2006.
- [2] Y. Cheng, Q. Fan, S. Pankanti, and A. Choudhary. Temporal sequence modeling for video event detection. In *IEEE Conference on Computer Vision and Pattern Recognition (CVPR)*, pages 2227–2234, 2014.
- [3] C. Dreher, N. Kulp, C. Mandery, M. Wchter, and T. Asfour. A framework for evaluating motion segmentation algorithms. In *2017 IEEE-RAS 17th International Conference on Humanoid Robotics (Humanoids)*, pages 83–90, 2017.
- [4] C. Feichtenhofer, A. Pinz, and A. Zisserman. Convolutional two-stream network fusion for video action recognition. In *2016 IEEE Conference on Computer Vision and Pattern Recognition (CVPR)*, pages 1933–1941, 2016.
- [5] D. Feldman, M. Monemizadeh, and C. Sohler. A PTAS for k -means clustering based on weak coresets. In *Proceedings of the 23rd ACM Symposium on Computational Geometry (SoCG)*, pages 11–18, 2007.
- [6] S. J. Gershman and D. M. Blei. A tutorial on bayesian nonparametric models. *Journal of Mathematical Psychology*, 56(1):1–12, 2012.
- [7] D. Gong, G. Medioni, S. Zhu, and X. Zhao. Kernelized temporal cut for online temporal segmentation and recognition. In *European conference on computer vision (ECCV)*, pages 229–243, 2012.
- [8] M. Hasan, J. Choi, J. Neumann, A. K. Roy-Chowdhury, and L. S. Davis. Learning temporal regularity in video sequences. In *IEEE Conference on Computer Vision and Pattern Recognition (CVPR)*, pages 733–742, 2016.
- [9] D. Huang, S. Yao, Y. Wang, and F. De La Torre. Sequential max-margin event detectors. In *European conference on computer vision (ECCV)*, pages 410–424, 2014.
- [10] M. C. Hughes and E. Sudderth. Memoized online variational inference for dirichlet process mixture models. In *Advances in Neural Information Processing Systems*, pages 1133–1141, 2013.
- [11] D. Jayaraman and K. Grauman. Slow and steady feature analysis: higher order temporal coherence in video. In *Proceedings of the IEEE Conference on Computer Vision and Pattern Recognition*, pages 3852–3861, 2016.
- [12] B. Krüger, A. Vögele, T. Willig, A. Yao, R. Klein, and A. Weber. Efficient unsupervised temporal segmentation of motion data. *IEEE Transactions on Multimedia*, 19(4):797–812, 2017.
- [13] H. Kuehne, J. Gall, and T. Serre. An end-to-end generative framework for video segmentation and recognition. In *IEEE Winter Conference on Applications of Computer Vision (WACV)*, pages 1–8, 2016.
- [14] G. Layher, T. Brosch, and H. Neumann. Real-time biologically inspired action recognition from key poses using a neuromorphic architecture. *Frontiers in Neurorobotics*, 11:13, 2017.

- [15] C. Lea, M. D. Flynn, R. Vidal, A. Reiter, and G. D. Hager. Temporal convolutional networks for action segmentation and detection. *arXiv preprint arXiv:1611.05267*, 2016.
- [16] S. Li, K. Li, and Y. Fu. Temporal subspace clustering for human motion segmentation. In *IEEE International Conference on Computer Vision (ICCV)*, pages 4453–4461, 2015.
- [17] Y. Li, C. Lan, J. Xing, W. Zeng, C. Yuan, and J. Liu. Online human action detection using joint classification-regression recurrent neural networks. In *European Conference on Computer Vision (ECCV)*, pages 203–220, 2016.
- [18] E. Liberty, R. Sriharsha, and M. Sviridenko. An algorithm for online k -means clustering. In *Proceedings of the Eighteenth Workshop on Algorithm Engineering and Experiments (ALENEX)*, pages 81–89, 2016.
- [19] M. Müller, T. Röder, M. Clausen, B. Eberhardt, B. Krüger, and A. Weber. Documentation mocap database HDM05. Technical Report CG-2007-2, Universität Bonn, 2007.
- [20] A. Y. Ng, M. I. Jordan, and Y. Weiss. On spectral clustering: Analysis and an algorithm. In *Advances in Neural Information Processing Systems 14*, pages 849–856. MIT Press, 2002.
- [21] D. Oneata, J. Verbeek, and C. Schmid. Action and event recognition with fisher vectors on a compact feature set. In *IEEE International Conference on Computer Vision (ICCV)*, pages 1817–1824, 2013.
- [22] R. Peng, H. Sun, and L. Zanetti. Partitioning well-clustered graphs: Spectral clustering works! *SIAM Journal on Computing*, 46(2):710–743, 2017.
- [23] X. Peng, L. Wang, X. Wang, and Y. Qiao. Bag of visual words and fusion methods for action recognition: Comprehensive study and good practice. *Computer Vision and Image Understanding*, 150:109–125, 2016.
- [24] H. Pirsiavash and D. Ramanan. Parsing videos of actions with segmental grammars. In *IEEE Conference on Computer Vision and Pattern Recognition (CVPR)*, pages 612–619, 2014.
- [25] A. Richard and J. Gall. Temporal action detection using a statistical language model. In *IEEE Conference on Computer Vision and Pattern Recognition (CVPR)*, pages 3131–3140, 2016.
- [26] K. Simonyan and A. Zisserman. Two-stream convolutional networks for action recognition in videos. In *Advances in neural information processing systems (NIPS)*, pages 568–576, 2014.
- [27] K. Soomro, A. R. Zamir, and M. Shah. Ucf101: A dataset of 101 human actions classes from videos in the wild. *arXiv preprint arXiv:1212.0402*, 2012.
- [28] K. Tang, L. Fei-Fei, and D. Koller. Learning latent temporal structure for complex event detection. In *IEEE Conference on Computer Vision and Pattern Recognition (CVPR)*, pages 1250–1257, 2012.
- [29] M. Tenorth, J. Bandouch, and M. Beetz. The TUM Kitchen Data Set of Everyday Manipulation Activities for Motion Tracking and Action Recognition. In *IEEE International Workshop on Tracking Humans for the Evaluation of their Motion in Image Sequences (THEMIS), in conjunction with ICCV2009*, 2009.
- [30] J. J. Verbeek, N. Vlassis, and B. Kröse. Efficient greedy learning of gaussian mixture models. *Neural computation*, 15(2):469–485, 2003.
- [31] U. von Luxburg. A tutorial on spectral clustering. *Statistics and Computing*, 17(4):395–416, 2007.
- [32] H. Wang and C. Schmid. Action recognition with improved trajectories. In *IEEE International Conference on Computer Vision (ICCV)*, pages 3551–3558, 2013.
- [33] L. Wiskott and T. J. Sejnowski. Slow feature analysis: Unsupervised learning of invariances. *Neural computation*, 14(4):715–770, 2002.
- [34] Y. Zhao, Y. Xiong, L. Wang, Z. Wu, X. Tang, and D. Lin. Temporal action detection with structured segment networks. *arXiv preprint arXiv:1704.06228*, 2017.
- [35] H. Zhong, J. Shi, and M. Visontai. Detecting unusual activity in video. In *IEEE Conference on Computer Vision and Pattern Recognition (CVPR)*, pages 819–826, 2004.
- [36] F. Zhou, F. De la Torre, and J. K. Hodgins. Hierarchical aligned cluster analysis for temporal clustering of human motion. *IEEE Transactions on Pattern Analysis and Machine Intelligence (PAMI)*, 35(3):582–596, 2013.
- [37] F. Zhou, F. D. la Torre, and J. K. Hodgins. Aligned cluster analysis for temporal segmentation of human motion. In *8th IEEE International Conference on Automatic Face and Gesture Recognition (FG)*, pages 1–7, 2008.